Pure appl. geophys. 161 (2004) 1185–1203
0033–4553/04/061185–19
DOI 10.1007/s00024-003-2493-y

Pure and Applied Geophysics

PART I: Theoretical Site Response Estimation for Microzoning Purposes

P. Triantafyllidis[1], P. Suhadolc[2], P. M. Hatzidimitriou[1], A. Anastasiadis[3], and N. Theodulidis[3]

Abstract — We estimate the theoretical site response along seven cross sections located in the city of Thessaloniki (Greece). For this purpose the 2-D structural models used are based on the known geometry and the dynamic soil properties derived from borehole measurements and other geophysical techniques. Several double-couple sources have been employed to generate the seismic wavefield, and a hybrid method that combines the modal summation with finite differences, has been deployed to produce synthetic accelerograms to a maximum frequency of 6 Hz for all components of motion. The ratios between the response spectra of signals derived for the 2-D local model and the corresponding spectra of signals derived for the 1-D bedrock reference model at the same site, allow us to estimate the site response due to lateral heterogeneities. We interpret the results in terms of both geological and geometrical features of the models and of the characteristics of the wave propagation. The cases discussed confirm that the geometry and depth of the rock basement, along with the impedance contrast, are responsible for ground amplification phenomena such as edge effects and generation and entrapment of local surface waves. Our analysis also confirms that the peak ground acceleration is not well correlated with damage and that a substantially better estimator for possible damage is the spectral amplification.

Key words: Site response, 2-D finite-differences modeling, hybrid method, spectral ratios, Thessaloniki, Greece.

Introduction

The destructive effects of the large earthquakes that occurred during recent years (e.g. Kobe 1995, Chi-Chi 1999, Izmit 1999), which mostly impacted urban areas with a heavy casualty toll, have fostered numerous studies on the estimation of seismic ground motion in a given urban area before the occurrence of a damaging earthquake. This task requires the detailed knowledge of both the subsurface structure within the city and of the probable location and characteristics of seismic sources around it. On the other hand, one needs theoretical methods and related computer codes that allow the simulation of the expected seismic ground motion. Detailed numerical simulations play an important role in

[1] Aristotle University, Geophysical Laboratory, P.O.Box 111, GR-54124 Thessaloniki, Greece.
[2] University of Trieste, Department of Earth Sciences, V. Weiss 1, I-34127 Trieste, Italy.
[3] Institute of Eng. Seismology and Earthq. Engineering (ITSAK), GR-55102 Thessaloniki, Greece.

the computation of ground motion, especially in areas of complex geology, because they can provide realistic synthetic waveforms at places where no recordings are available. Synthetics are compared with observations wherever instrumental data are available, in order to validate and, if needed, to further improve the theoretical techniques. Consequently, during recent years several methods have been proposed for the theoretical estimation of seismic response at a specific site (e.g., FÄH and SUHADOLC, 1994; FURUMURA and TAKENAKA, 1996; WALD and GRAVES, 1998; FIELD *et al.*, 2000).

The theoretical methods that study the wave equation can be classified (e.g., FÄH *et al.*, 1993; SUHADOLC, 1997) into two sizable categories: numerical and analytical methods. Numerical methods make use of grid techniques, i.e., the discretization of the medium and the derivatives (in time and space) of the wave equation and subsequent solution of the derived system of linear equations. In analytical methods, differential equations and boundary conditions are translated into integral equations that are discretized and solved by using various mathematical techniques. Analytical methods usually require as input data models with simple geometries, as opposed to numerical methods which are more suitable to process relatively complex structures, even if restricted by the size of the model due to limitations of computer memory.

In this study we extend the work of TRIANTAFYLLIDIS *et al.* (1998), who applied the hybrid method and derived preliminary results for two of the cross sections, to a total of seven cross sections located within the city of Thessaloniki.

Method

The hybrid method employed in this work for the construction of synthetics is throughly described in other papers (FÄH, 1992; FÄH and SUHADOLC, 1994; FÄH *et al.* 1994; PANZA *et al.*, 2000). It combines two techniques: finite differences (FD) and modal summation (MS). The structural model used in the computations consists of two parts: A simple 1-D "bedrock" or "regional" structure and a 2-D lateral heterogeneous structure. The source is located in the 1-D structure and the calculations are performed in two stages. The seismic wavefield is propagated from the source to the boundaries of the laterally heterogeneous area applying the MS method. The time series that result from this technique are used to excite the wave propagation in the laterally heterogeneous medium and the seismic wavefield is propagated with the FD technique. The hybrid approach thus allows the calculation of the local seismic wavefield for short (few kilometers) as well as for long (several hundred kilometers) epicentral distances. The use of the MS method also permits the study of extended sources which can be modeled as a sum of point sources properly distributed in time and space, allowing the simulation of a realistic rupture process at the causative fault (e.g., SARAÒ *et al.*, 1998; BAJC *et al.*, 2001).

Even if currently relatively powerful computers with considerable memory are available, there will always be memory limitations in the use of the FD method. The need to study wave propagation either for spatially very extended areas or at high frequencies ($f > 5\,\mathrm{Hz}$) is becoming in fact increasingly greater. To ascertain that spurious reflections from the artificial boundaries of the FD grid in space have been properly treated, we initially compare the results from the MS computation with those from FD for the simple case of the 1-D regional velocity model. The 2-D simulations are only performed if the differences between the above results vary within 2–5%.

Data and Process

Our 2-D simulations are based on detailed geotechnical information originating from a series of tests and extended geophysical prospects (cross-hole and down-hole measurements, surface-wave inversions) carried out within the entire urban area of Thessaloniki by the Laboratory of Soil Mechanics and Foundation Engineering of Aristotle University of Thessaloniki. The known geometry and the dynamic properties of the soil (density, body-wave velocities and quality factors) that were used resulted from various studies of this area (PITILAKIS *et al.*, 1992; ANASTASIADIS, 1994; RAPTAKIS, 1995).

All information has been elaborated in order to construct seven 2-D cross sections, each one along a profile with different orientation (Fig. 1), covering most of the city area.

After the selection of the location of each profile, all available information on subsurface layer properties derived from existing bore-holes in the surroundings (RAPTAKIS *et al.*, 1994; PITILAKIS and ANASTASIADIS, 1998) were projected on the related section. In such a way, also by stratigraphically correlating between the adjacent bore-holes, 2-D cross sections have been constructed. Apart from the geometry of the layering, which was rather well constrained by data, all dynamic layer properties (densities, body wave velocities, quality factors) were estimated by RAPTAKIS (1995). The 2-D local velocity models along each of the seven profiles were thus constructed, their thickness varying according to the depth of the solid bedrock. Each such local velocity model is underlain by a common "regional" velocity model derived from the studies of the wider area of the Serbomacedonian geological zone (LIGDAS and LEES, 1993; PAPAZACHOS, 1998) to which the city area belongs. Consequently, the local 2-D velocity model overlies the regional 1-D model, consisting of homogeneous, horizontal and anelastic layers. The layering of the seven cross sections, as well as each layer dynamic properties, are shown in detail by TRIANTAFYLLIDIS *et al.* (2004) (PART-II, this volume).

The focal mechanisms of the double-couple point sources that were used to excite the seismic wavefield impingent on the cross sections and allowing the construction of the 2-D synthetic accelerograms, are shown in Table 1. The fault

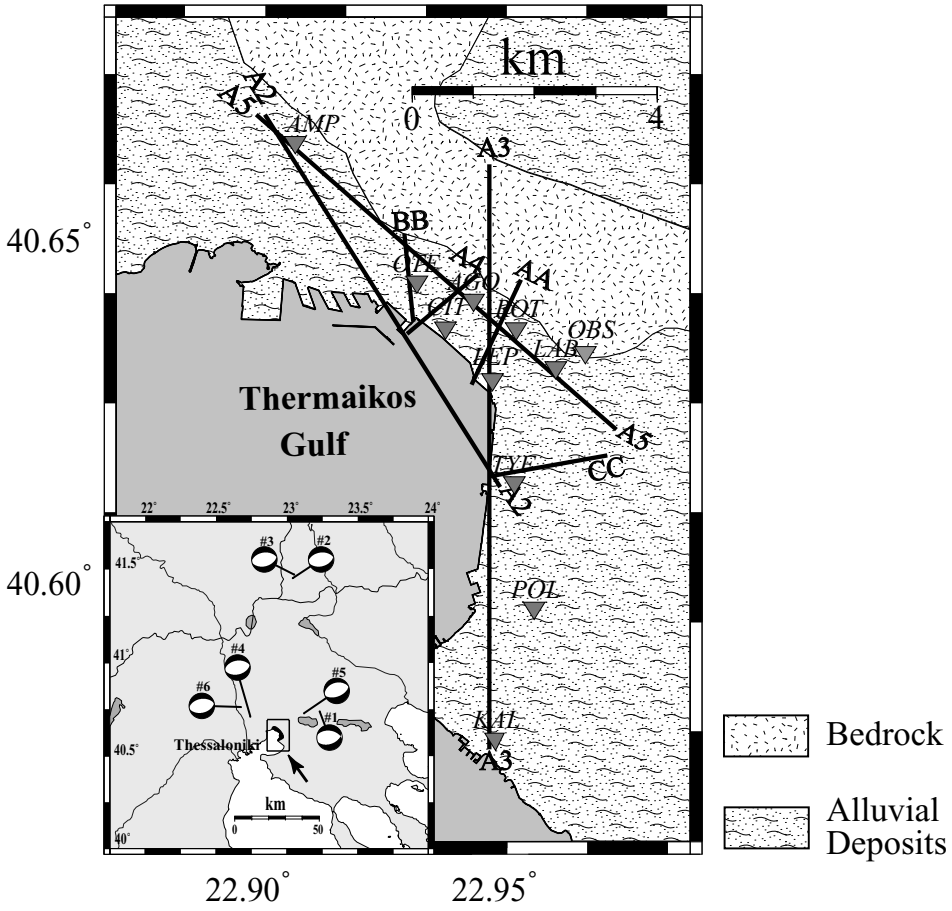

Figure 1
Map of Thessaloniki and the cross sections along which the seismic response (site effects) is estimated through the hybrid method (see text). In the inset, the focal mechanisms of the simulated events are shown, while the arrow denotes the area under investigation.

Table 1

Parameters of earthquakes used for the construction of synthetic accelerograms.

No.	Date	Long.°	Lat.°	M_S	Depth (km)	Strike	Dip	Rake
1.	780620	40.740°	23.230°	6.5	6.0	278°	46°	−70°
2.	931222	41.450°	23.040°	3.3	7.0	76°	45°	−94°
3.	931216	41.470°	23.050°	4.7	7.0	76°	45°	−94°
4.	940108	40.712°	22.742°	2.5	6.0	76°	45°	−94°
5.	780704	40.730°	23.120°	5.1	6.0	252°	37°	−88°
6.	940216	40.764°	22.676°	2.0	5.0	76°	45°	−94°

plane solution of source #1 (Table 1) corresponds to that of the destructive earthquake ($M_s = 6.5$) of June 20, 1978, whereas source #5 corresponds to its largest aftershock ($M_s = 5.1$) of July 4. The fault plane solutions used for sources #2, #3, #4 and #6 (Table 1), are representative of the active stress field in the area of northern Greece according to PAPAZACHOS and KIRATZI (1996).

In Table 2 we report some parameters of the seven sections that were used: the first column shows the section's code name, whereas the second one gives the event number (see Table 1). The third column gives the distance between the source and the first virtual receiver in the 2-D grid; the fourth column gives the interval between the receivers along the section. The fifth and sixth columns show the length of the FD grid in the horizontal and vertical dimensions, respectively.

In order to estimate the seismic motion allowing for the lateral heterogeneities, the hybrid method (FÄH, 1992) was applied for the construction of two sets of synthetic accelerograms along each section. The first set was calculated by assuming that the receivers are placed on the 1-D regional velocity model, whereas the second set is obtained by placing the receivers on top of the local 2-D velocity model. The two simulations were performed for all components of motion for a maximum calculation frequency of 6 Hz. In order to check the accuracy of the 2-D computations, the synthetics that resulted from the hybrid method when using the 1-D regional velocity model were compared with the ones that came out from the application of the purely analytical MS method for the same model. The amplitude differences were always less than 5%, an acceptable value (FÄH, 1992), and a confirmation of the validity of the boundary conditions applied in the hybrid method. The site response (or site effects) along the profiles is (are) estimated through spectral ratios. For each receiver along the section, the spectrum of the synthetic accelerogram calculated using the local 2-D model is divided by the respective synthetic spectrum obtained at the same receiver with computations performed using the 1-D regional model.

Table 2

Technical characteristics of the seven sections used as input to the application of hybrid method.

Section	Source used	Source distance (km)	Receivers interval (m)	FD grid dimensions (m)	
				Horizontal	Vertical
AA	#2	90.60	35	1300	5075
BB	#3	91.43	30	1300	6120
CC	#1	26.46	30	1500	6318
A2	#4	15.45	81	7100	6480
A3	#2	89.67	81	7700	6375
A4	#5	17.22	30	1400	8970
A5	#6	23.70	90	7000	10230

Results

In Figure 2 we show an example of the hybrid method results: the synthetic accelerograms obtained along the 2-D local velocity model of section A5. The time origin of the accelerograms is the instant in which the seismic waves enter the FD grid. The waveforms have been normalized per component to the amplitude of the waveform with the maximum Peak Ground Acceleration (PGA).

From the synthetics it is possible to extract the variation of some ground motion related quantities along the 2-D local velocity section, such as peak ground acceleration, PGA(2D), and Arias intensity, W(2D). Arias intensity is defined as

$$W = \frac{\pi}{2g} \int_0^\infty [\ddot{x}(T)]^2 \, dt \ ,$$

where, x, is the ground displacement, g, the gravity acceleration, t, the time and, T, the motion duration (Arias, 1970). Dots indicate differentiation in time.

In order to eliminate as much as possible the effects of source and regional propagation, the two quantities PGA(2D) and W(2D) are normalized to the quantities PGA(1D) and W(1D), respectively. The latter are calculated for the regional 1-D velocity model and the normalization performed for each receiver. In this way, the calculation of the relative peak ground acceleration, PGA(2D)/PGA(1D), and the relative Arias intensity, W(2D)/W(1D), allows the estimation of 2-D site response as compared with the site response obtained from the 1-D laterally homogeneous regional velocity model. Figures 3a and 3b show the variation of the above quantities along all sections for the radial (up), transverse (middle) and vertical (bottom) components. The variation of PGA(2D)/PGA(1D) is shown with a dashed line and is measured on the left vertical axis, whereas W(2D)/W(1D) is given as a continuous line and is measured on the right vertical axis. As can be expected from the definition of W, this quantity presents high values at those points along the models where the synthetic waveforms have high amplitudes and long durations.

Along section AA, the relative PGA and Arias intensity have their highest values (2.5 to 5), especially for the radial component, at a distance of 91 km from the seismic source at the transition from bedrock to alluvium. An analogous observation was made by FÄH and SUHADOLC (1994) as well as MARRARA and SUHADOLC (1998) for the city of Benevento, and the explanation was sought in the lateral high impedance between the superficial layers and rocky bedrock (edge effect), giving rise to the excitation of local surface waves. Something similar occurs for section BB, the

►

Figure 2
An example of the hybrid method results: the three component synthetic accelerograms computed for the local 2-D model along section A5 (Table 2) with a maximum calculation frequency of 6 Hz.

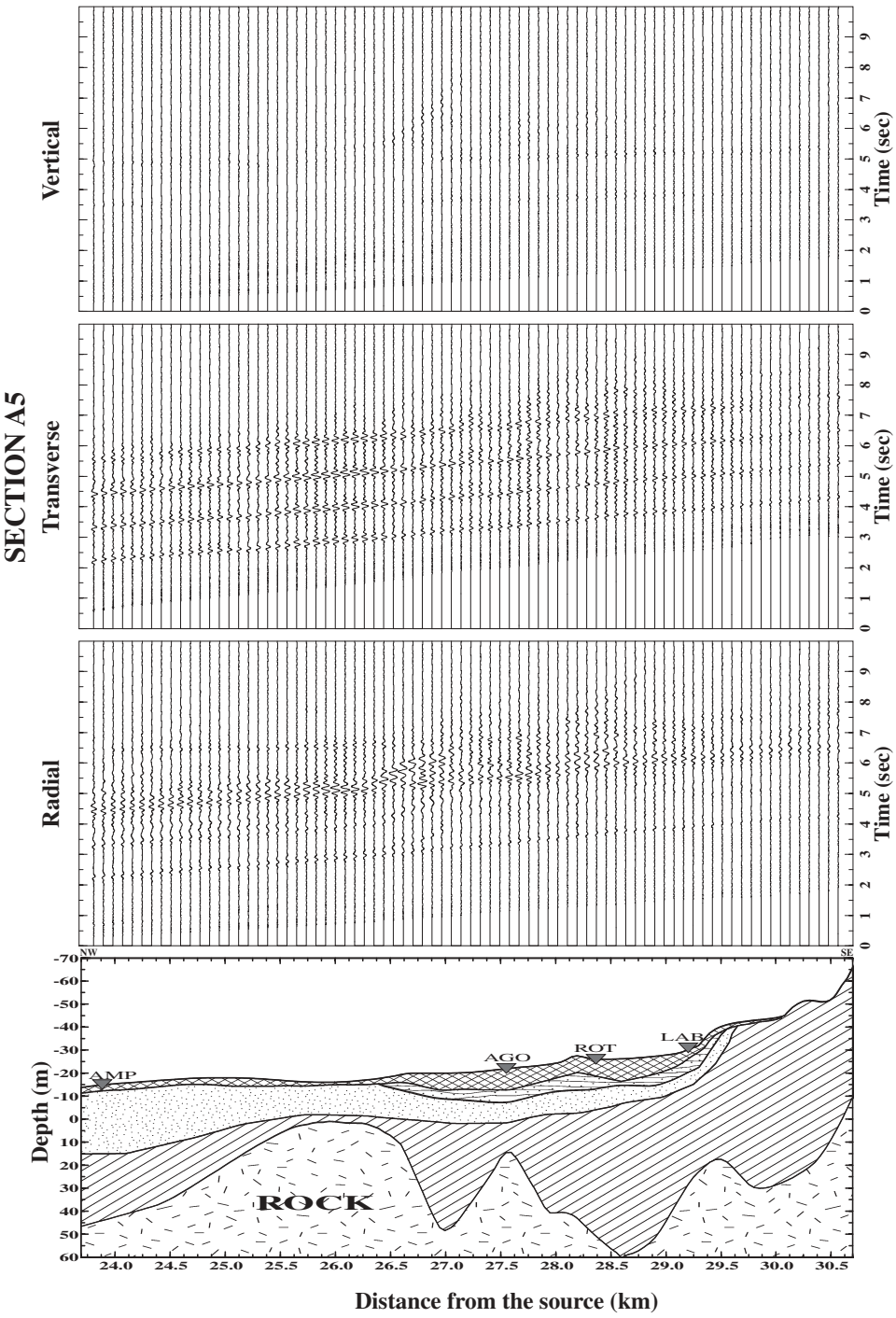
SECTION A5
Vertical
Transverse
Radial
Time (sec)
NW
SE
AMP
AGO
ROT
LAB
ROCK
Depth (m)
Distance from the source (km)

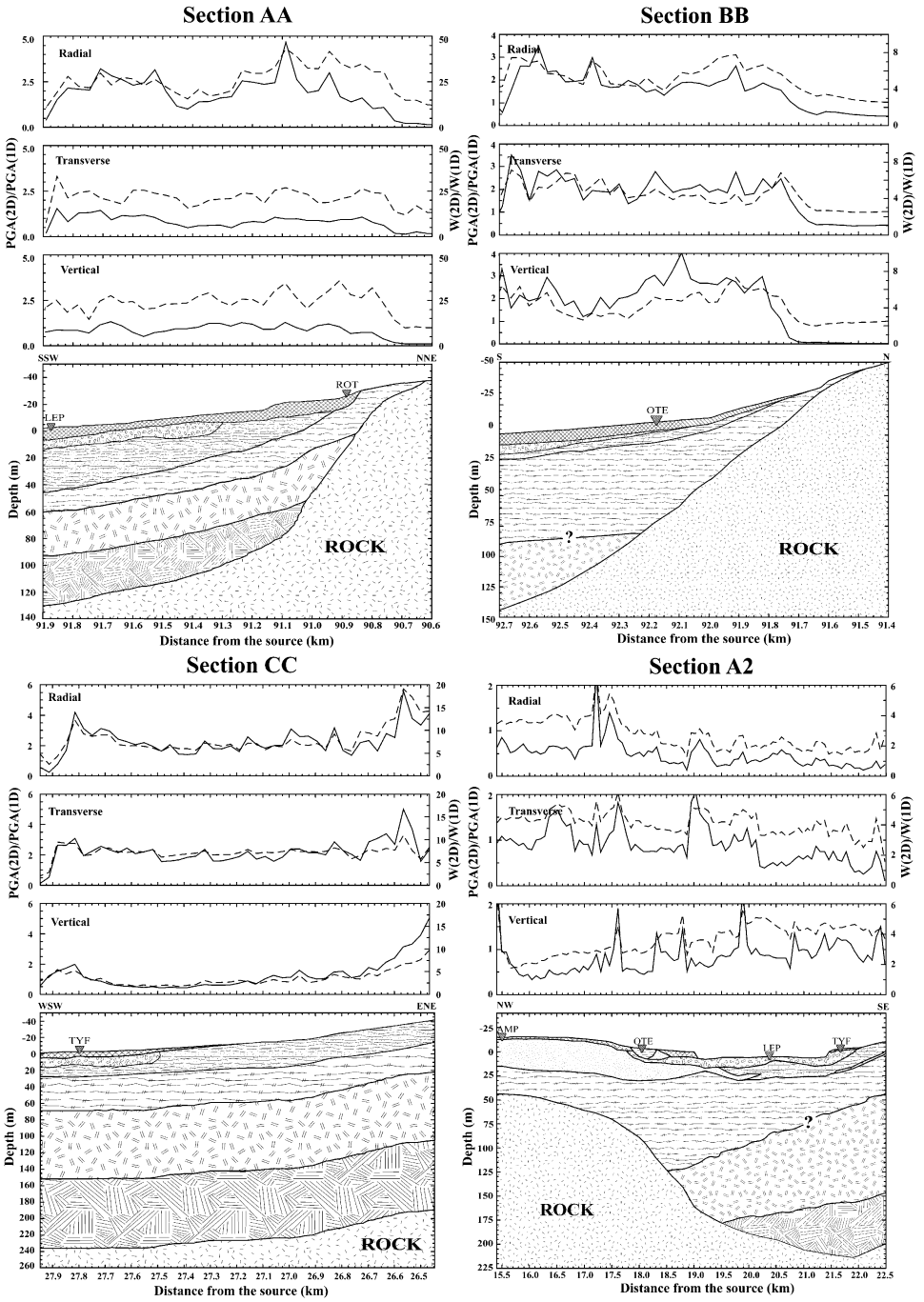
Section AA
Radial
Transverse
Vertical
PGA(2D)/PGA(1D)
W(2D)/W(1D)
SSW
NNE
LEP
ROT
Depth (m)
ROCK
Distance from the source (km)
Section BB
Radial
Transverse
Vertical
PGA(2D)/PGA(1D)
W(2D)/W(1D)
S
N
OTE
?
ROCK
Depth (m)
Distance from the source (km)
Section CC
Radial
Transverse
Vertical
PGA(2D)/PGA(1D)
W(2D)/W(1D)
WSW
ENE
TYF
ROCK
Depth (m)
Distance from the source (km)
Section A2
Radial
Transverse
Vertical
PGA(2D)/PGA(1D)
W(2D)/W(1D)
NW
SE
AMP
OTE
LEP
TYF
?
ROCK
Depth (m)
Distance from the source (km)

maximum of relative PGA and Arias intensity appearing close to the position of station OTE (Fig. 3a). Low values of these quantities are characteristic, especially for the vertical component, for the part of the model where the bedrock approaches the surface. At the other edge of the basin, slightly increased values of PGA(2D)/PGA(1D) and W(2D)/W(1D) are observed, which are probably due to the boundary conditions that delimit the artificial basin boundaries. Similar boundary effects are also seen on the ENE side of section CC (Fig. 3a), despite the simple geometry of the profile giving rise to stable values of PGA and W. Sections A2 (Fig. 3a) and A3 (Fig. 3b) have a relatively complex subsurface structure giving rise to high values of PGA(2D)/PGA(1D) and W(2D)/W(1D) at distances of 17.5 km and 90.5 km from the seismic source, respectively. Especially for the case of section A3 (Fig. 3b), the edge effect is very intense, causing high ground accelerations particularly for the vertical component, as denoted by the values of relative PGA (Fig. 3b) that exceed 4. Very strong edge effect at the discontinuity between the basin and the solid bedrock is noticed close to the area of station AGO on section A4. Conversely, in the part of the model which is closer to the seismic source (17.2 to 17.5 km), as well as in the deeper parts of the basin (18.2 to 18.6 km), the acceleration amplitudes for the 2-D model are relatively low (Fig. 3b), giving values of PGA(2D)/PGA(1D) below 1 for the three components. It is worth noting that at CIT the values of PGA(2D)/PGA(1D) and W(2D)/W(1D) are relatively low, despite the position of this site located only about half a kilometer away towards the center of the basin. At the site CIT, located over a thick package of sediments, strong damage had been observed during the earthquake of June 20, 1978. This only confirms that quantities such as PGA or duration of motion provide only a crude estimation of seismic motion and that they are not very good indicators of damage potential (e.g., FÄH and SUHADOLC, 1994).

The synthetic accelerograms of section A5 (Fig. 2) are very characteristic and the observed waveforms reflect the complex geometry of the 2-D model and particularly the bedrock surface anomalies. The waveforms over the small basin part of the model with the thick sedimentary layers (distances between 28 km and 29.5 km from the source) show high durations due to the trapped energy both within the superficial layers and in the basin with local surface waves generated. On the other end, the already mentioned edge effect might be responsible for the high values of PGA(2D)/PGA(1D) and W(2D)/W(1D) in the area where the bedrock rises to very shallow depths (25.5 km to 26.5 km from the seismic source), especially for the transverse component (Fig. 3b).

Other ground motion related quantities, which also can be extracted from the synthetics that were estimated with the numerical simulation for the 2-D local

◄

Figure 3a
Variation of quantities PGA(2D)/PGA(1D) (thin line) and W(2D)/W(1D) (thick line) along sections AA, BB, CC and A2 for all components of motion. The ratio PGA(2D)/PGA(1D) is measured on the left and W(2D)/W(1D) is measured on the right axis.

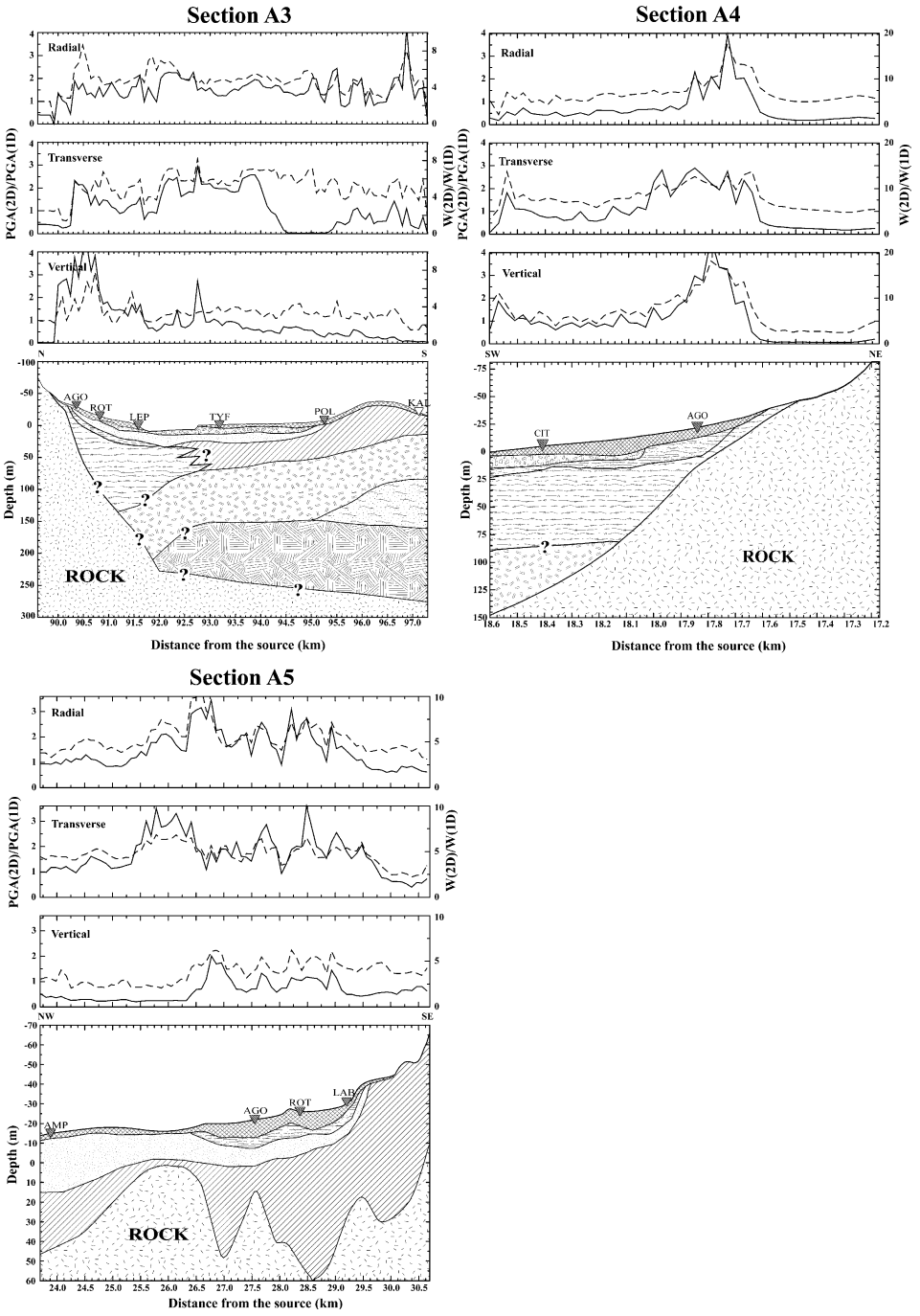

Figure 3b
The same as Figure 3a but for sections A3, A4 and A5.

velocity model, are the Fourier Amplitude Spectrum, FAS(2D), and the Spectral acceleration, Sa(2D), or response spectrum. In order to estimate the above quantities that are due only to the heterogeneities of the local velocity model, we normalized them to the respective quantities FAS(1D) and Sa(1D), as they were calculated for the 1-D regional velocity model with the hybrid method for the given source-receiver distance. By this normalization, the effects of the radiation pattern and propagation in the regional model were reduced and the results obtained reflect the effect of the 2-D local model on the seismic motion. In Figure 4 the variation with frequency of the ratio FAS(2D)/FAS(1D) is shown, indicatively only for section BB and Figure 5 (a and b) displays the ratios Sa(2D)/Sa(1D) between spectra with 5% damping for all components of motion along all the profiles.

The quantity FAS(2D)/FAS(1D) is estimated at ten selected sites on the surface of each section. The selection of these sites has been made based on the geometry and the layer parameters of each profile. In other words we proceeded to check all those points where the local soil profile has interesting features. Wherever along the profile a seismometer [RefTek station] was placed that recorded some event (LACHET *et al.*, 1996), the ratio FAS(2D)/FAS(1D) was computed also at those locations.

The variation with frequency of the ratio Sa(2D)/Sa(1D) between spectra with 5% damping is presented in color for all three components of motion along each section. The white spots that appear at some profiles indicate amplifications that are slightly higher than the maximum value specified on the color scale of each section. For section AA (Fig. 5a) the radial component is generally more amplified than the other two for all frequencies, and the highest values of amplification are observed for frequencies below 3 Hz. Moreover, low amplifications are observed in the middle of the basin at frequencies smaller than 4.5 Hz for all components. This indicates that the spectral amplification obtained from the 2-D local model is only a few times higher than the 1-D regional model amplification for these specific epicentral distances and azimuthal positions.

In the same figure, the simple geometry of section's BB bedrock interface is outlined. At distances from 91.75 km to 92.2 km from the seismic source, the amplification of the vertical component is high for frequencies above 3 Hz. Moving over the center to the basin edge (92.5–92.8 km from source), all components' spectral amplifications become high. This increase of spectral amplification for the horizontal components appears at frequencies 1 to 3 Hz, whereas for the vertical component it is less intense and appears at higher frequencies (3 to 5 Hz).

In the next graph of Figure 5a the horizontal layering and the relatively simple geometry of section CC produce, as expected, rather simple results. The radial component presents slightly higher amplifications than the other two. Actually, there are no important differences observed between the spectral amplification due to 2-D local and 1-D regional velocity models in the entire basin area. Close to site TYF (27.65 km, approximately) the vertical component amplification is low enough, while for the horizontal one it is significantly higher.

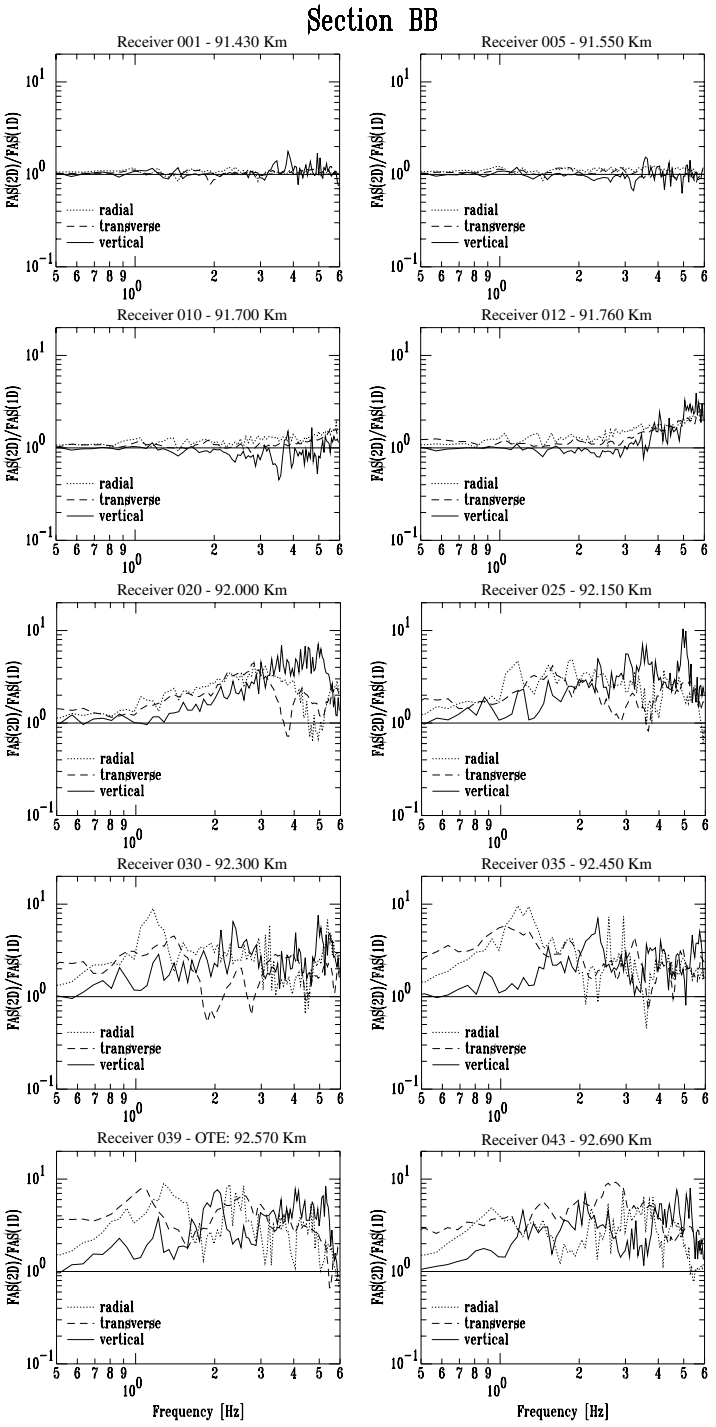
Section BB
Receiver 001 - 91.430 Km
Receiver 005 - 91.550 Km
Receiver 010 - 91.700 Km
Receiver 012 - 91.760 Km
Receiver 020 - 92.000 Km
Receiver 025 - 92.150 Km
Receiver 030 - 92.300 Km
Receiver 035 - 92.450 Km
Receiver 039 - OTE: 92.570 Km
Receiver 043 - 92.690 Km
FAS(2D)/FAS(1D)
radial
transverse
vertical
Frequency [Hz]

In the final graph of Figure 5a, where the variation of Sa(2D)/Sa(1D) along section A2 is presented, it seems that at distances approaching 18.5 km from the seismic source, where the layer geometry is horizontal, the amplification for all components, in particularly the vertical one, is quite low. The only exception is the radial component for frequencies ranging 1 to 1.5 Hz. For distances (> 18.6 km) farther from the seismic source, where the geology is more complex, the amplification appears at higher frequencies, and this is probably due to the effect of the thin superficial layers.

In the first graph of Figure 5b, the high amplification zones (up to 92 km) outline the interface between bedrock and basin boundaries of section A3, especially for the horizontal components. At the basin's center, between sites TYF and POL (93 to 95 km) a zone of increased amplification appears at different frequencies for each component. For the radial component the maximum amplification is recognized between 0.5 Hz and 2.5 Hz, whereas for the transverse component the maximum is seen between 1.5 Hz and 4 Hz. The vertical component has high amplifications at the same distances from the source, but for much higher frequencies (5 to 6 Hz) and are unevenly distributed. These high amplifications at high frequencies can be attributed to local surface waves which are trapped in the layers close to the surface. The spectral amplifications along section A4 have a very similar frequency variation in space and the level is approximately the same for all three components (Fig. 5b). At site AGO (about 17.9 km from the source) the values of amplification are relatively low for frequencies less than 3 Hz, but reach values ranging from 4 to 6 for higher frequencies. Very high values of amplification, especially for horizontal components, appear close to the area of CIT (around 18.4 km from the source) and exceed the value of 9 at frequencies mainly below 3 Hz. The low amplitude of the ratio PGA(2D)/PGA(1D) computed at the same site (Fig. 3b) contrasts with the above results. As mentioned earlier this can be explained by the fact that PGA(2D)/PGA(1D) is a frequency-independent quantity. Therefore, it is evident from the figure that the amplification of spectral acceleration occurs at different frequencies for the sites CIT and AGO. Combining this observation with the extent of damage in the area around CIT during the earthquake of June 20, 1978, the importance of estimating spectral amplifications for earthquake engineering purposes is evident. The knowledge of site response in relation to the complete frequency content of a specific design earthquake is therefore the only reliable image of seismic hazard useful for engineers.

The last graph of Figure 5b shows the variation of Sa(2D)/Sa(1D) along section A5. The bedrock configuration is clearly evidenced at distances 25.5 to

◄

Figure 4
Variation of ratio FAS(2D)/FAS(1D) at selected sites indicatively along section BB for radial (dotted), transverse (dashed) and vertical component (continuous line).

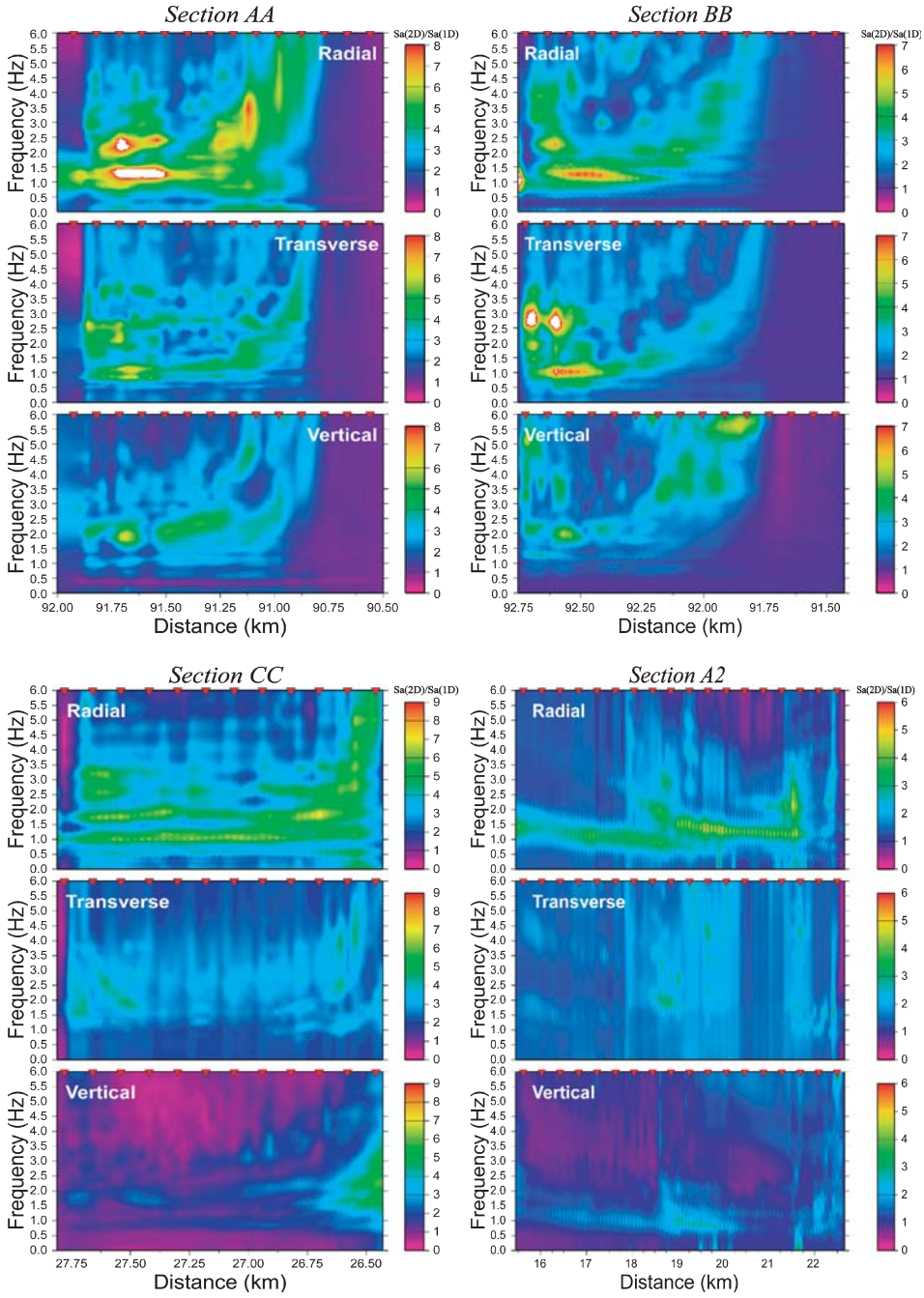

Figure 5a
Colored presentation of the Sa(2D)/Sa(1D) ratio with frequency, along sections AA, BB, CC and A2 (spectra computed with 5% dumping) for all three components.

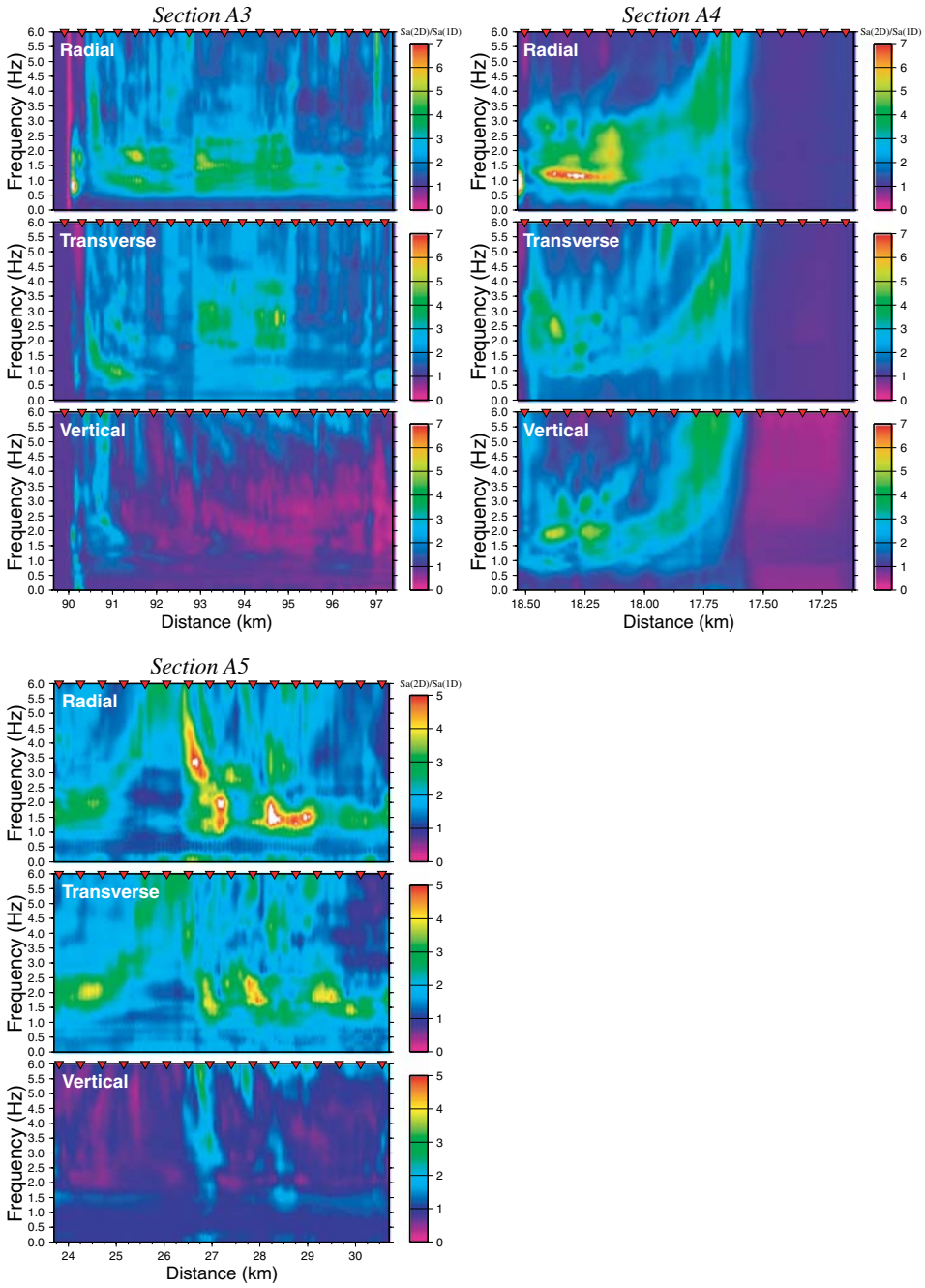

Figure 5b
The same as Figure 5a, but for sections A3, A4 and A5.

26.5 km from the source by low values of amplification at low frequencies for both horizontal components, with essentially no amplification on the vertical component. Along the points where the total width of the sedimentary layers increases (from 26.5 km on), the horizontal components appear to be strongly amplified between 1 and 2 Hz. On the contrary, the vertical component generally shows low amplifications that vanish at higher frequencies. This is probably due to the presence of the clay layer below the superficial alluvial deposits, which amplifies the vertical component of the surface waves producing high amplifications only at frequencies exceeding 4.5 Hz.

Conclusions

We have used the seismic waves propagation in non-homogeneous media to estimate the maximum expected seismic amplification at selected points within the city of Thessaloniki. The hybrid method proposed by FÄH (1992) has been used, taking into account the 2-D geometry and the variation of dynamic parameters along different cross sections crossing the city area with different orientations. The conclusions are compendiously presented in the following paragraphs.

Generally, the very low cost and the high computational speed make the 1-D methods for site response estimation useful in geologically simple regions with low seismicity, where usually no experimental data exists. However, in places where the subsurface geology pattern is complicated, this simple approach is not sufficient, as demonstrated by, e.g., TRIANTAFYLLIDIS *et al.* (1998) and MARRARA and SUHADOLC (2001). Thus, the use of at least a 2-D numerical simulation is required to acquire reliable estimations of seismic motion amplification. In the event strong motion observations are available, it is of course possible to have discordances between theoretical and experimental estimations of site effects. This is mainly due to two reasons: a) unavailability of a sufficiently detailed knowledge of the large number of parameters that characterize the input model and b) the neglecting of possible 3-D effects.

The cases we have discussed in this paper confirm that the geometry and depth of the rock basement are important factors that can significantly affect the seismic amplification of a certain site (see section A5 in Fig. 5b). In cases where the rock basement is located at shallow depths under the surface, the major differences of impedance between the surface layers and the basement generate edge effects (see section A3 in Fig. 5b). It has also been observed that the thin low-velocity surface layers generate resonance and entrap local surface waves, thereby creating increased amplifications (generally between 1 and 4 Hz) for the horizontal components, whereas the vertical component is only amplified at higher (over 5 Hz) frequencies. This phenomenon is particularly evident in sections BB, A3 and A5 (Figs. 5a and 5b).

We have also demonstrated that, in some cases, the value of the PGA alone does not constitute a reliable measure of seismic motion amplification. For instance, at site AGO of section A4 the relative PGA values are higher than those at site CIT, although the latter is located in the center of the basin where the thickness of the underlying sediments is higher. However, the spectral amplification (Sa) values at these two sites are significantly different from each other, thus explaining the different levels of damage caused by the 1978 earthquake at these two sites.

The proposed 2-D models based on the geotechnical and geophysical investigations explain quite well the main amplification features at the area of interest. Such detail in the knowledge of the subsurface structure can be, therefore, considered as sufficient, within the related frequency range, to reliably estimate for engineering purposes the ground motion shaking effects within a city, given a scenario earthquake.

Purposeful to making the results applicable for antiseismic planning and the mitigation of seismic hazard, with emphasis on large urban areas such as the city of Thessaloniki, the next step (e.g. FÄH *et al.*, 1993; PANZA *et al.*, 2001) is to employ such results to construct microzoning maps for each scenario earthquake.

Acknowledgements

This work has been financially supported and performed within the framework of the following projects: "Progetto Finalizzato Beni Culturali, CNR, Italy," UNESCO-IUGS-IGCP project 414 and EU project "EVG1-CT-2001-00040."

REFERENCES

ANASTASIADIS, A. (1994), *Contribution to the Study and the Determination of Dynamic Properties of Typical Greek Soils*, Ph.D. Thesis (in Greek), Dept. of Civil Eng., Aristotle Univ. of Thessaloniki, pp. 1–389.

ARIAS, A., *A measure of earthquake intensity*. In (R. J. Hansen, ed.) *Seismic Design for Nuclear Power Plants*, (MIT Press, Cambridge, Massachusetts 1970), pp. 438–483.

BAJC, J., AOUDIA, A., SARAÒ, A., and SUHADOLC, P. (2001), *The 1998 Bovec-Krn Mountain* (*Slovenia*) *Earthquake Sequence*, Geophys. Res. Lett. *28*, 1839–1842.

FÄH, D. (1992), *A Hybrid Technique for the Estimation of Strong Ground Motion in Sedimentary Basins*, Ph.D. Thesis, Nr 9767, Swiss Federal Institute of Technology, Zürich.

FÄH, D., IODICE, C., SUHADOLC, P., and PANZA, G. F. (1993), *A New Method for the Realistic Estimation of Seismic Ground Motion in Megacities: The Case of Rome*, Earthquake Spectra *9*, 643–668.

FÄH, D., and SUHADOLC, P. (1994), *Application of Numerical Wave-propagation Techniques to Study Local Soil Effects: The Case of Benevento* (*Italy*), Pure Appl. Geophys. *143*, 513–536.

FÄH, D., SUHADOLC, P., MUELLER, St., and PANZA, G. F. (1994), *A Hybrid Method for the Estimation of Ground Motion in Sedimentary Basin: Quantitative Modeling for Mexico City*, Bull. Seismol. Soc. Am. *84*, 383–399.

FIELD, E. H., and the SCEC PHASE III WORKING GROUP (2000), *Accounting for Site Effects in Probabilistic Seismic Hazard Analyses of Southern California: Overview of the SCEC Phase III Report*, Bull. Seismol. Soc. Am. *90*, 6B, S1–S31.

FURUMURA, T., and TAKENAKA, H. (1996), *2.5-D Modeling of Elastic Waves Using the Pseudospectral Method*, Geophys. Res. Lett. *25*, 785–788.

LACHET, C., HATZFELD, D., BARD, P. Y., THEODULIDIS, N., PAPAIOANNOU, C., and SAVVAIDIS, A. (1996), *Site Effects in the City of Thessaloniki* (*Greece*). *Comparison of Different Approaches*, Bull. Seismol. Soc. Am. *86*, 1692–1703.

LIGDAS, C. N., and LEES, J. M. (1993), *Seismic Velocity Constraints in the Thessaloniki and Chalkidiki Areas* (*Northern Greece*) *from a 3-D Tomographic Study*, Tectonophysics *228*, 97–121.

MARRARA, F., and SUHADOLC, P. (1998), *Site Amplifications in the City of Benevento* (*Italy*)*: Comparison of Observed and Estimated Ground Motion from Explosive Source*, J. of Seismol. *2*, 125–143.

MARRARA, F., and SUHADOLC P. (2001), *2-D Modeling of Site Effects along the "EURO-SEISTEST" Array* (*Volvi Graben*, *Greece*), Pure Appl. Geophys. *158*, 12, 2369–2388.

PANZA, G. F., and SUHADOLC, P., *Complete strong motion synthetics*. In *Seismic Strong Motion Synthetics*, Computational Techniques *4* (B. A. Bolt, eds.), (Orlando, Academic Press (1987)), pp. 153–204.

PANZA, G. F., ROMANELLI, F., and VACCARI, F. (2000), *Seismic Wave Propagation in Laterally Heterogeneous Anelastic Media: Theory and Applications to Seismic Zonation*. Advances in Geophysics *43*, 1–95.

PANZA, G. F., VACCARI, F., and ROMANELLI, F. (2001), *Realistic Modeling of Seismic Input in Urban Areas: A UNESCO-IUGS-IGCP Project*, Pure Appl. Geophys. *158*, 12, 2389–2406.

PAPAZACHOS, C. B. (1998), *Crustal P- and S-velocity Structure of the Serbomacedonian Massif* (*Northern Greece*) *Obtained by Non-linear Inversion of Travel Times*, Geophys. J. Int. *134*, 25–39.

PAPAZACHOS, C. B., and KIRATZI, A. A. (1996), *A Detailed Study of the Active Crustal Deformation in the Aegean and Surrounding Area*, Tectonophysics *253*, 129–153.

PITILAKIS, K., MARGARIS, B., LEKIDIS, V., THEODOULIDIS, N., and ANASTASIADIS, A. (1992), *The Griva*, *Northern Greece*, *Earthquake of December 21*, *1990*, *Seismological*, *Structural and Geotechnical Aspects*, J. of Eur. Earthq. Eng. *2*, 20–35.

PITILAKIS, K., and ANASTASIADIS, A. (1998), *Soil and Site Characterization for Seismic Response Analysis*, Proc. 11th ECEE, 65–90, Paris 6–11 September, France.

RAPTAKIS, D. (1995), *Contribution to the Determination of the Geometry and the Dynamic Properties of Soil Formations and their Seismic Response*, Ph.D. Thesis (in Greek), Dept. of Civil Eng., Aristotle Univ. of Thessaloniki.

RAPTAKIS, D., KARAOLANI, E., PITILAKIS, K., and THEODULIDIS, N. (1994), *Horizontal to Vertical Spectral Ratio and Geological Conditions: The Case of a Downhole Array in Thessaloniki* (*Greece*), Proc. XXIV Gen. Ass. ESC, Athens, Greece 3, 1570–1578.

SARAÒ, A., DAS, S., and SUHADOLC, P. (1998), *Effect of Non-uniform Station Coverage on the Inversion for Earthquake Rupture History for a Haskell-type Source Model*, J. Seismol. *2*, 1–25.

SUHADOLC, P. (1997), *Local Effects on Strong Ground Motion: Basic Physical Phenomena and Estimation Methods for Microzoning Studies*, Proc. of the Advanced Study Course on Seismic Risk "SERINA", 21–27 Sept., 1997, Thessaloniki, Greece, 229–299.

TRIANTAFYLLIDIS, P., HATZIDIMITRIOU, P. M., SUHADOLC, P., THEODULIDIS, N., and PITILAKIS, K. (1998), *Comparison between 1-D and 2-D Site Effects Modeling in Thessaloniki*, Proc. 2nd International Symposium on: *The Effects of Surface Geology on Seismic Motion*, 1–3 Dec., 1998, Yokohama, Japan, 2, 981–986.

TRIANTAFYLLIDIS, P., HATZIDIMITRIOU, P. M., THEODULIDIS, N., SUHADOLC, P., PAPAZACHOS, C., RAPTAKIS, D., and LONTZETIDIS, K. (1999), *Site Effects in the City of Thessaloniki* (*Greece*) *Estimated from Acceleration Data and 1-D Local Soil Profiles*, Bull. Seismol. Soc. Am. *89*, 521–537.

TRIANTAFYLLIDIS, P. A., HATZIDIMITRIOU, P. M., and SUHADOLC, P. (2001), *1-D Theoretical Modelling for Site Effect Estimations in Thessaloniki - Comparison with Observations*, Pure Appl. Geophys. *158*, 12, 2333–2347.

TRIANTAFYLLIDIS, P., HATZIDIMITRIOU, P. M., SUHADOLC, P., THEODULIDIS, N., and ANASTASIADIS, A. (2004), *PART-II: Comparison of Theoretical and Experimental Site Effect Estimation Results*, Pure Appl. Geophys. *161*, 1205–1219.

WALD, D. J., and GRAVES, R. W. (1998), *The Seismic Response of the Los Angeles Basin*, *California*, Bull. Seismol. Soc. Am. *88*, 337–356.

(Received February 25, 2002, accepted November 18, 2002)